LEXINGTON LABORATORIES, INC.
Cambridge, Mass. 02140

DEVELOPMENT OF PIGMENTS FOR THERMAL CONTROL COATINGS

by

Philip S. Schaffer - Lexington Laboratories, Inc.
David W. Jones - Lexington Laboratories, Inc.

GPO PRICE $ _____

Contract Number NAS8-20162
(908-20-02-0147)

CFSTI PRICE(S) $ _____

Hard copy (HC) 3.00

Microfiche (MF) .50

ff 653 July 65

George C. Marshall Space Flight Center
National Aeronautics and Space Administration
Huntsville, Alabama 35812

April, 1966

LEXINGTON LABORATORIES, INC.
Cambridge, Mass. 02140

DEVELOPMENT OF PIGMENTS FOR THERMAL CONTROL COATINGS

FINAL REPORT

by

Philip S. Schaffer - Lexington Laboratories, Inc.
David W. Jones - Lexington Laboratories, Inc.

Contract Number NAS8-20162
(908-20-02-0147)

George C. Marshall Space Flight Center
National Aeronautics and Space Administration
Huntsville, Alabama 35812

April, 1966

FOREWORD

This is the final report on the program, "Development of Pigments for Thermal Control Coatings", conducted for George C. Marshall Space Flight Center, National Aeronautics and Space Administration, under Contract No. NAS8-20162 covering the period from 17 June 1965 to 16 December 1965. The principal investigator for this program was Philip S. Schaffer; the research engineer was David W. Jones. W. B. Campbell was instrumental in initiating the program and provided consultation through a portion of the work. The program originated from prior Lexington Laboratory studies aimed at producing Al_2O_3 whiskers and powders by gas phase reactions.

35-226

ABSTRACT

The feasibility of producing powders of alumina (Al_2O_3), zirconia (ZrO_2), silica (SiO_2), titania (TiO_2), zinc oxide (ZnO) and zinc titanate ($ZnTiO_3$) by homogeneous nucleation in the vapor phase was determined. The general reaction used, whereby a metal chloride was initially formed by flowing a controlled amount of chlorine gas over a metal source, then reacted with controlled amounts of carbon dioxide and hydrogen gases, is shown:

$$MCl_{2x}(g) + xCO_2(g) + xH_2(g) \rightleftharpoons MO_x(s) + xCO(g) + 2xHCl(g)$$

Appropriate growth parameters for the individual materials were determined, although optimum process variables for obtaining particular particle sizes were not established.

Samples prepared did not have unusual radiation stability, but the capability of producing powders of extremely uniform particle size and of controlled composition was demonstrated.

TABLE OF CONTENTS

LIST OF FIGURES

LIST OF TABLES

1.0 INTRODUCTION

The objective of this program was to study the feasibility of producing a variety of oxide pigments by vapor-phase reaction that would be available for space-stable thermal-control coatings. Powders for this application should possess a low ratio of solar absorptance to infrared emittance and also exhibit high stability to electromagnetic radiation encountered in the space environment. The performance of a pigment may be affected by such variables as particle size, particle size distribution, purity and degree of crystal perfection. Thus, these factors have received particular attention.

The formation of powders by homogeneous nucleation from vapor phase reactions offers several advantages over other methods of preparation. These include (a) control of impurity species and attainment of high purity levels, (b) control of particle size by blending for optimum concentrations relative to the light input spectrum and (c) low defect concentration since mechanical size reduction is not required and powders are formed isothermally.

In the present study no attempt was made to prepare large quantities of pigment materials nor to attain particular levels of purity. The major goal was to determine the breadth of the techniques applicability to a variety of materials and to determine its advantages and disadvantages relative to other methods of powder preparation.

2.0 TECHNICAL BASIS

The technical basis for the method used lies in the experimental observation that in a flowing stream of reactant gases from which a solid oxide phase is precipitated, the morphology of the solid formed (powder, bulk crystal, platelet or whisker) is determined by temperature, supersaturation, gas composition, pressure and flow conditions[1-4]. For an overall reaction such as:

$$2AlCl_3(g) + 3H_2(g) + 3CO_2(g) \rightleftharpoons Al_2O_3(s) + 3CO(g) + 6HCl(g) \quad (1)$$

it is believed that the actual gas phase reaction is of the general form:

$$2AlCl_3(g) + 3H_2(g) + 3CO_2(g) \rightleftharpoons 3CO(g) + 6HCl(g) + O_2(g) + Al_2O(g) \quad (2)$$

followed by condensation:

$$O_2(g) + Al_2O(g) \rightleftharpoons Al_2O_3(s) \quad (3)$$

Gas reaction equilibrium is achieved rapidly relative to condensation and nucleation of the solid phase. Thus the gas phase reaction equilibrium constant is given by:

$$K = \frac{P_{CO}^3 \; P_{HCl}^6 \; P_{O_2} \; P_{Al_2O}}{P_{CO_2}^3 \; P_{H_2}^3 \; P_{AlCl_3}^2} \quad (4)$$

For non-equilibrium condensation, the tendency for nucleation and condensation depends on the supersaturation ratio of the species involved in the condensation process:

$$\Sigma_T = \frac{(P_{O_2}\ P_{Al_2O})\ \text{actual}}{(P_{O_2}\ P_{Al_2O})\ \text{equil.}} = K^{-1}\left[\frac{P_{CO}^3\ P_{HCl}^6}{P_{CO_2}^3\ P_{H_2}^3\ P_{AlCl_3}^2}\right] \quad (5)$$

Thus, by controlling the temperature, the total system pressure and the gas composition, (which determine K), the supersaturation can be controlled.

For homogeneous nucleation a high value of the supersaturation ratio is required, but once this necessary level is achieved the nucleation process occurs rapidly[5]. When nuclei are formed, they grow at a rate which is determined by the supersaturation ratio and by the kinetics of the specific surface reactions and deposition processes involved. The length of time that particles are allowed to grow, and thus their final size can be controlled by the reactant gas velocity which is determined by furnace dimensions, temperature, pressure and flow rates.

Detailed knowledge of the actual reaction mechanisms involved is not known, but the direction in which changing process variables affects results can be predicted and is the technical basis for an empirical study of the feasibility of applying the method to a number of systems.

The vapor train and furnace assembly used for these oxide powder growth studies is shown schematically in Figure 1. Reactant gases, chlorine (99.5% purity), pre-purified hydrogen (99.9% purity), carbon dioxide (99.5% purity), and C. P. carbon monoxide (99.5% purity) were passed through

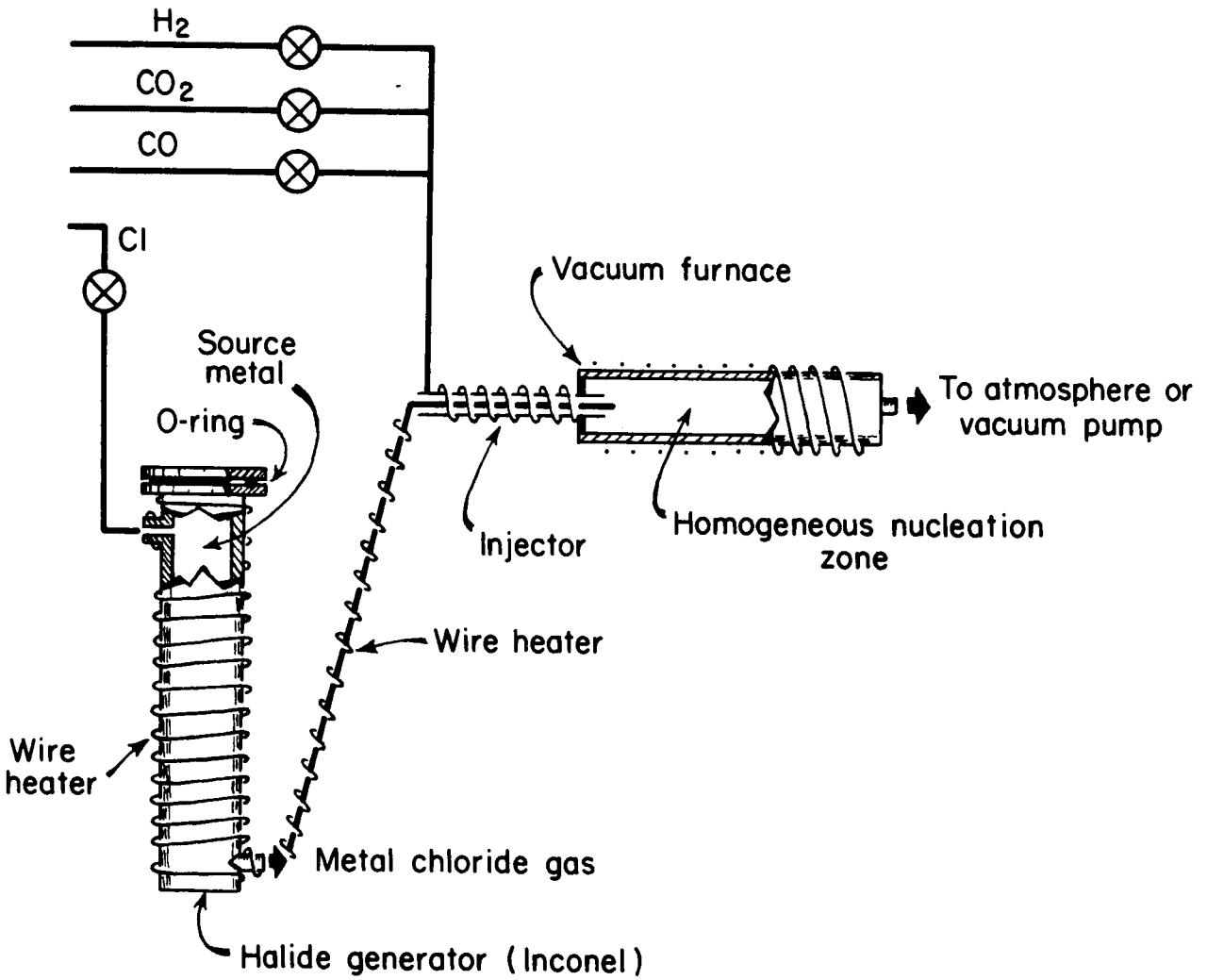

Figure 1: Schematic Diagram of Homogenous Nucleation Apparatus.

anhydrous calcium sulfate drying chambers. Hydrogen was also passed through a catalytic purifier to remove oxygen. All gases were then passed through flow meters and into the reaction chamber via an injection tube. Gaseous reaction products were removed and system pressure maintained with an appropriate vacuum pumping system as described previously[6].

Metal chloride vapor was generated in a temperature controlled chamber by chlorination of the metal, according to the following general reaction:

$$M(s) + xCl_2(g) \rightleftharpoons MCl_{2x}(g) \qquad (6)$$

This method was previously developed[6] to permit direct control of the chloride vapor pressure rather than depending upon the sublimation of the chloride at a controlled temperature. This method also precluded the necessity of a carrier gas.

After formation, the metal chloride vapor was passed through transfer lines maintained at a temperature which prevented condensation. The vapor entered the reaction chamber where it was mixed with the other reactant gases, hydrogen, carbon dioxide (and carbon monoxide when used), in the hot zone of the furnace, producing the metal oxide powder by the following general overall reaction:

$$MCl_{2x}(g) + xCO_2(g) + xH_2(g) \rightleftharpoons MO_x(s) + xCO(g) + 2xHCl(g) \qquad (7)$$

A hydrogen protected, molybdenum-element furnace capable of operating at temperatures up to 1850°C was used to externally heat a 2.2 cm inside diameter alumina (99.7% Al_2O_3) tube. At the exhaust end of the reaction chamber, a sight port was located which allowed observation of powder fall

during operation. Furnace wall temperature was measured with a calibrated optical pyrometer and controlled with a variable transformer. Condensable reaction gases were removed in a liquid nitrogen trap, while others were exhausted through the vacuum pumping system. Aluminum oxide was produced in a 4.5 cm inside diameter tube while all other oxides were produced in 2.2 cm inside diameter alumina tubes.

3.0 RESULTS AND DISCUSSION

Results obtained are discussed separately for each of the materials investigated.

3.1 Alumina (Al_2O_3) Powder Preparation

Aluminum oxide powders were prepared by the overall chemical reaction:

$$2AlCl_3(g) + 3H_2(g) + 3CO_2(g) \rightleftharpoons Al_2O_3(s) + 3CO(g) + 6HCl(g) \quad (1)$$

The aluminum chloride was generated by passing a controlled flow of chlorine gas over aluminum metal in the form of 99.99% purity 0.020-inch thick sheet at a temperature of 400°C. This temperature provided complete reaction.

$$Al(s) + \frac{3}{2} Cl_2(g) \rightleftharpoons AlCl_3(g) \quad (7)$$

At this temperature the product has the composition $AlCl_3$[7] so that the aluminum chloride flow rate is two-thirds that of the chlorine introduced. Transfer lines were maintained at 220°C to prevent condensation of the aluminum chloride in transit to the reaction chamber.

Based on previous observations of powder morphology a number of runs were made (some of which were reported previously[1,2]) at fixed reactant flow rates but with varying reaction chamber temperature, total pressure and gas velocities, as shown in Table 1:

TABLE 1: Conditions for the Formation of Al_2O_3 Powder*

Sample No.	System Pressure (Torr)	Temp. °C	Gas Velocity (cm/sec)	Time in Hot Zone (sec.)	Tube Inside Diam. (cm)
Al_2O_3 - 1	50	1750	147	6.8×10^{-2}	5.5
Al_2O_3 - 2	760	1800	354	2.8×10^{-2}	1.0
Al_2O_3 - 3	15	1800	2,077	4.8×10^{-3}	2.2
Al_2O_3 - 4	50	1700	1,020	9.8×10^{-3}	2.2
Al_2O_3 - 5	50	1750	147	6.8×10^{-2}	5.5

*Input gas flow rates: CO_2 - 0.20 liters/min; CO - 0.80 liters/min; H_2 - 0.80 liters/min; $AlCl_3$ - 0.12 liters/min.

3.2 Alumina (Al_2O_3) Powder Characteristics

Only small samples of powders Al_2O_3 - 2, Al_2O_3 - 3, and Al_2O_3 - 4 were prepared. These were examined by electron microscopy, x-ray diffraction and x-ray line broadening to determine powder characteristics[1]. A larger sample of powder, Al_2O_3 - 1, was prepared and examined by optical microscopy (oil immersion), centrifugal sedimentation particle size determination and spectrochemical analysis. Sample characteristics are shown in Table 2.

TABLE 2: Al_2O_3 Powder Characteristics

Sample	Crystal Structure	Particle Size (microns)
Al_2O_3 - 1	α-Al_2O_3	0.36 - 3.5 (Sedimentation, optical microscopy)
Al_2O_3 - 2	α-Al_2O_3, γAl_2O_3	0.1 (x-ray, electron microscopy)
Al_2O_3 - 3	ND	0.02-0.04 (x-ray, electron microscopy)
Al_2O_3 - 4	ND	0.02-0.06 (x-ray, electron microscopy)
Al_2O_3 - 5	α-Al_2O_3	0.29 (avg) (optical microscopy)

The crystal structure of the alumina powder is fixed by the reaction temperature. At temperatures above about 1150°C, α-Al_2O_3 (corundum) is formed. Various lower temperature forms (gamma, eta, theta), not precisely identified result below this temperature.

The particle size of the product depends both on the reaction chamber temperature and supersaturation ratio which determine the crystal growth rate, and on the gas velocity determined by temperature, pressure, flow rate and furnace dimensions which fixes the growth time. Changing residence time in the hot zone from 68 milliseconds at 1750°C to 9.8 milliseconds at 1700°C changes the average particle size by about an order of magnitude. One of the unique characteristics of the process is that the growth times are exceedingly short, orders of magnitude shorter than other reaction systems, and thus a remarkable uniformity in particle size material, Al_2O_3 - 1, results as shown in Figure 2. A photomicrograph of one of the powders is shown in Figure 3.

In the present experiments, no exhaustive efforts were made to prepare exceedingly high purity powders. In Table 3 spectrochemical analyses are shown of the Al_2O_3 - 1 powder, the aluminum metal reacted to form $AlCl_3$ and the alumina reaction chamber:

TABLE 3: Qualitative Spectrochemical Analysis (ppm)

Powder Al_2O_3 - 1		Al Metal	Reaction Chamber
B	< 1	ND	ND
Na	1 - 10	ND	$10 - 10^2$
Mg	1 - 10	$1 - 10^2$	$10 - 10^2$
Ca	1 - 10	< 1	$10^3 - 10^4$
Si	ND	1 - 10	$10^3 - 10^4$
Mn	1 - 10	ND	10

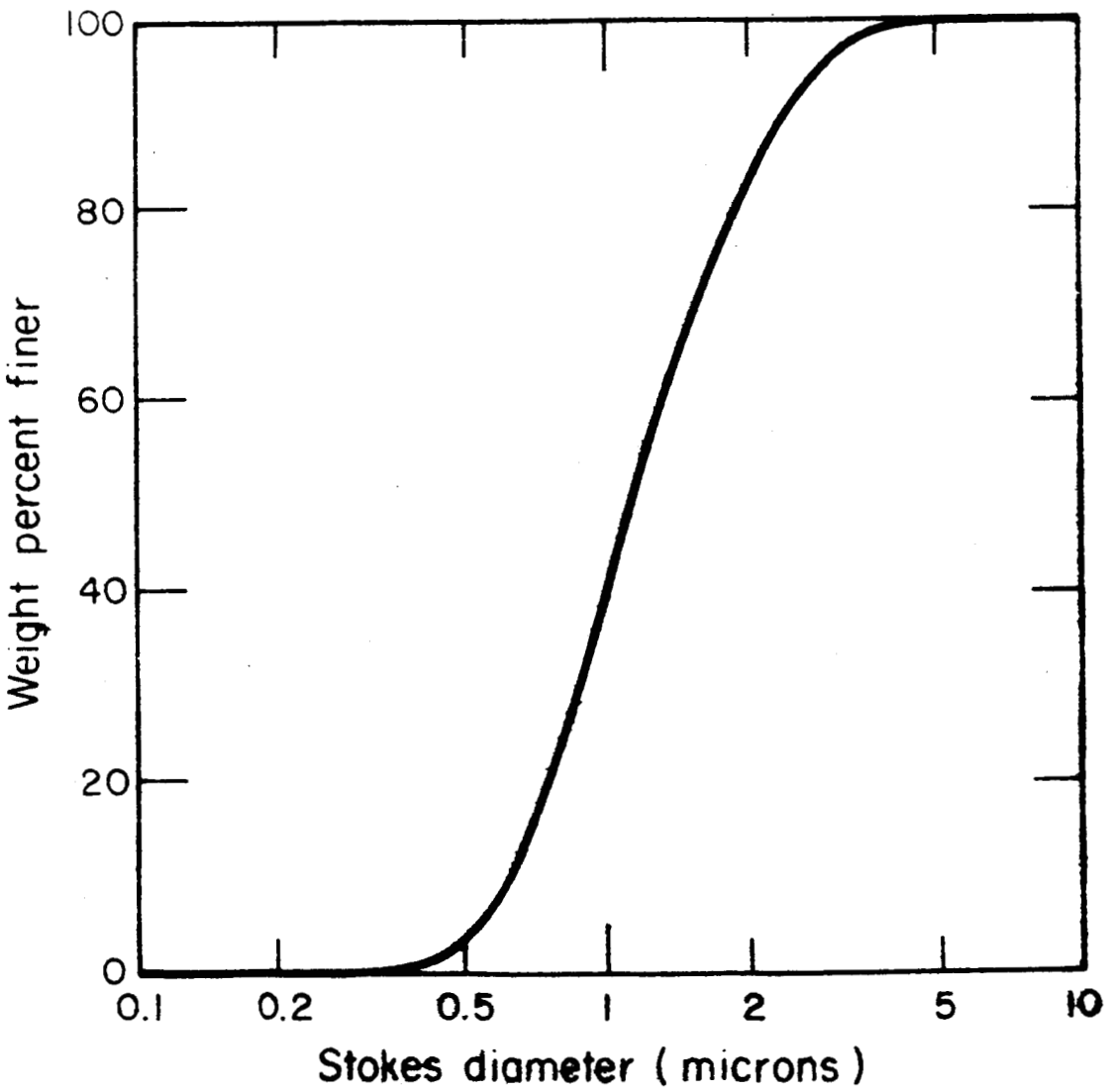

Figure 2: Particle Size Distribution of Al_2O_3 Powder Formed by Homogeneous Nucleation.

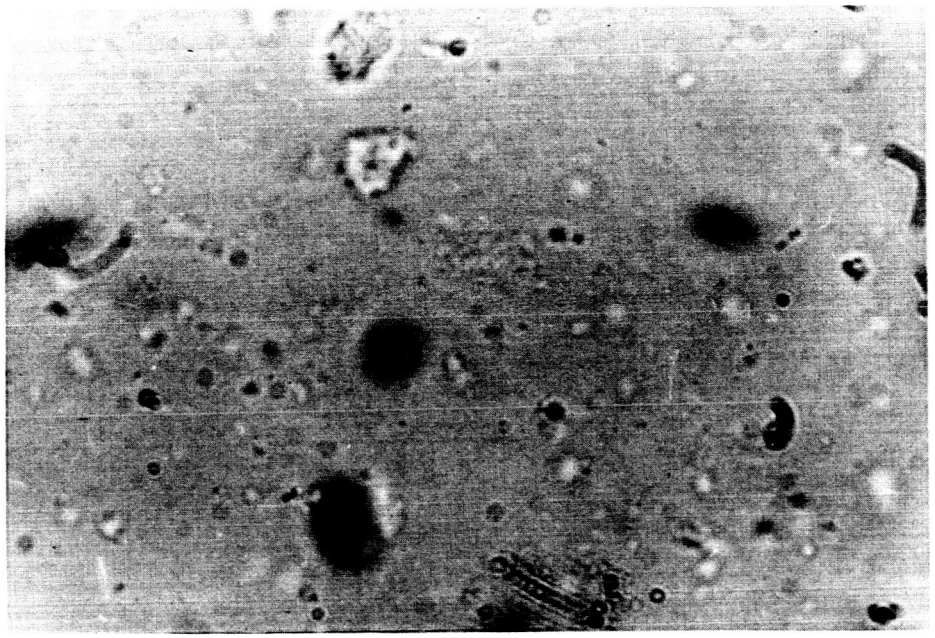

Figure 3: Photomicrograph of Al_2O_3 - 5 Powder Sample (4,026x; avg. particle size 0.29 microns; avg. agglomerate size, 4mm).

Fe	$10^2 - 10^3$	< 1	$10^2 - 10^4$
Ni	$10 - 10^3$	ND	10
Cu	$10 - 10^2$	< 1	1
Ga	< 1	ND	ND
Mo	$10 - 10^2$	ND	ND
Ag	< 1	< 1	ND
Sn	$10 - 10^2$	< 1	ND
Cr	$10^3 - 10^4$	ND	$10^3 - 10^4$ (estimated)*
Pb	ND	1 - 10	10

*Thin light pink coating of $Cr:Al_2O_3$ on surface of reaction chamber.

Copper, nickel and tin concentrations are greater in the powder sample than in the starting material or reaction chamber; they are believed to come from the heated $AlCl_3$ transfer lines.

In contrast to results found for single crystal growth[6] where the vapor-formed product was of greater purity than the starting materials and furnace chamber, the powder product clearly grows with the inclusion of those impurities present in the vapor stream. This result is to be expected under the conditions of rapid nucleation and growth employed and indicates that considerable care is required to prepare extremely high purity powders. It also shows that intentionally-introduced concentrations of most elements can readily be incorporated in the powder product.

3.3 Zirconia (ZrO_2) Powder Preparation

Zirconium dioxide powders were prepared by the overall chemical reaction:

$$ZrCl_4(g) + 2H_2(g) + 2CO_2(g) \rightleftharpoons ZrO_2(s) + 2CO(g) + 4HCl(g) \quad (8)$$

The zirconium tetrachloride was generated by passing a controlled flow of chlorine gas over zirconium metal at 400°C.

$$Zr(s) + 2Cl_2(g) \rightleftharpoons ZrCl_4(g) \quad (9)$$

The sublimation temperature of zirconium tetrachloride is 300°C; transfer lines were maintained at 400°C to insure that there would be no condensation of the zirconium tetrachloride in transit to the reaction chamber. The chlorination temperature provided complete reaction.

The temperature of the growth chamber was maintained at 1550°C to produce the high-temperature monoclinic form, baddeleyite. At this temperature the oxide was formed but there was an admixture of zirconium tetrachloride in the product unless an excess of hydrogen was used. Conditions for the formation of zirconia powder are shown in Table 4. A range of total pressures and corresponding gas velocities were investigated with those shown in Table 4 resulting in uniform powder production. Changing the relative flow rates of reaction constituents resulted in powders ranging in color from dark grey to metallic. Conditions shown in Table 4 resulted in white deposits.

TABLE 4: Conditions for the Production of ZrO_2 Powder

Sample	System Pressure (Torr)	Temp. °C	Gas Velocity (cm/sec)	Time in Hot Zone (sec.)
ZrO_2	60	1550	484	2×10^{-2}

3.4 Zirconia (ZrO_2) Powder Characteristics

Only small samples were prepared. These were examined by x-ray diffraction, optical microscopy and spectrochemical analysis. Sample characteristics are shown in Table 5, and a photomicrograph of the powder is shown in Figure 4.

TABLE 5: Characteristics of ZrO_2 Powder

Sample	Crystal Structure	Particle Size Microns
ZrO_2	Major - monoclinic Minor - cubic	< 0.5 μ (optical microscopy)

The major phase found to be present was the monoclinic form of zirconia, baddeleyite, having a refractive index of 2.2. X-ray diffraction of the powder sample, Fig. 5, shows that an additional constituent, believed to be cubic zirconia, was present in minor amounts.

Spectrochemical analysis of the powder formed, metal used and alumina furnace tube are shown in Table 6. The major contaminant in the powder was aluminum oxide introduced from the furnace tube. Other constituents identified in the powder were in the range less than 10 ppm. Particle size was measured by optical examination (Fig. 4), and the average particle size was 0.22 microns.

3.5 Silica (SiO_2) Powder Formation

Silicon dioxide powder was prepared by the following general reaction:

$$SiCl_4(g) + 2H_2(g) + 2CO_2(g) \rightleftharpoons SiO_2(s) + 2CO(g) + 4HCl \quad (10)$$

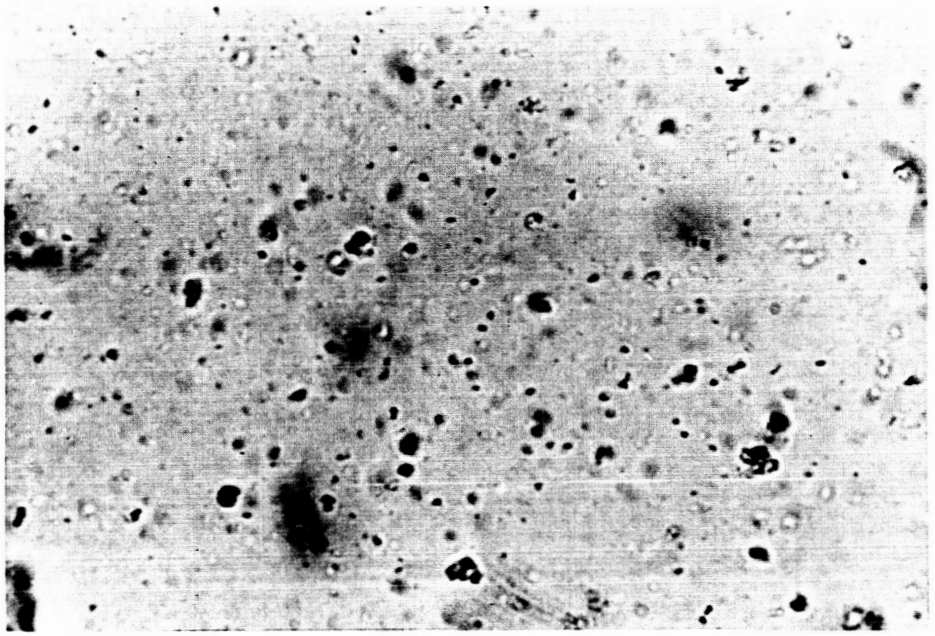

Figure 4: Photomicrograph of ZrO_2 Powder Sample (4,026x; avg. particle size 0.22 microns)

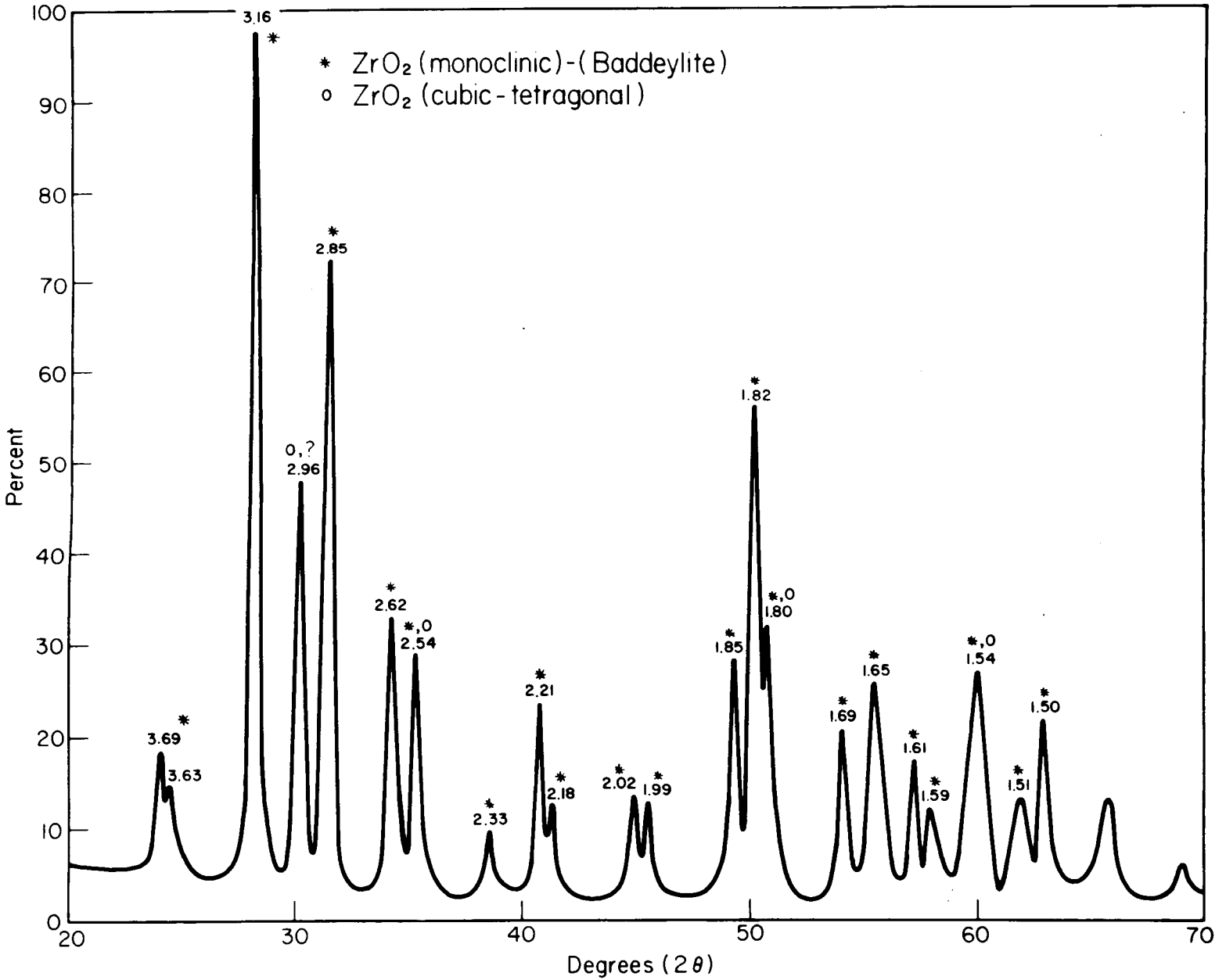

Figure 5: Phase Determination of Zirconium Dioxide by X-Ray Diffraction. Intensity vs. 2θ.

TABLE 6: Qualitative Spectrochemical Analysis of ZrO_2 Powder (ppm)

Element	Powder	Source Metal	Reaction Tube
Be	< 1	ND	ND
B	< 1	< 1	ND
Na	ND	ND	$10 - 10^2$
Mg	ND	2×10^2	$10 - 10^2$
Al	$10^3 - 10^4$	< 20	Remainder Al_2O_3
Si	1 - 10	< 50	$10^3 - 10^4$
Ca	1 - 10	ND	$10^3 - 10^4$
Ti	ND	< 20	10
V	ND	< 20	1
Cr	1 - 10	98	10
Mn	1 - 10	< 50	10
Fe	1 - 10	6×10^2	$10^2 - 10^4$
CO	ND	< 10	ND
Ni	1 - 10	ND	10
Cu	1 - 10	ND	1
Zi	Remainder ZrO_2	Remainder Zr	ND
Sn	1 - 10	ND	ND
Hf	ND	91	ND
Hg	ND	ND	1
Pb	1 - 10	< 20	10

The silicon tetrachloride was generated by passing a flow of chlorine gas over silicon metal at a temperature of 400°C. This temperature provided complete reaction.

$$Si(s) + 2Cl_2(g) \rightleftharpoons SiCl_4 \qquad (11)$$

At this temperature the product has a composition $SiCl_4$ so that the chloride flow rate is half that of the chlorine introduced. Transfer lines were maintained at 200°C to prevent condensation of the silicon chloride in transit to the reaction chamber.

The growth chamber was maintained at a temperature of 1550°C; at this temperature the cristobalite form of silica is stable. Conditions used for SiO_2 powder formation are shown in Table 7. During several experimental runs to establish conditions for effective powder preparation, it was noted that the alumina reaction tube acquired a glazed appearance indicating reaction with the vapor stream.

TABLE 7: Conditions for the Production of SiO_2 Powder

Sample	System Pressure (Torr)	Temp. °C	Gas Velocity (cm/sec)	Time in Hot Zone (sec)
SiO_2	60	1550	375	2.7×10^{-2}

3.6 Silica (SiO_2) Powder Characteristics

Small amounts of silica powder were prepared. These were examined optically and by spectrochemical analysis. Optical observations indicated that the particle size ranged from 0.30 to 0.59 microns in diameter as shown in Fig. 6. The powder was white and had an index of refraction of 1.484

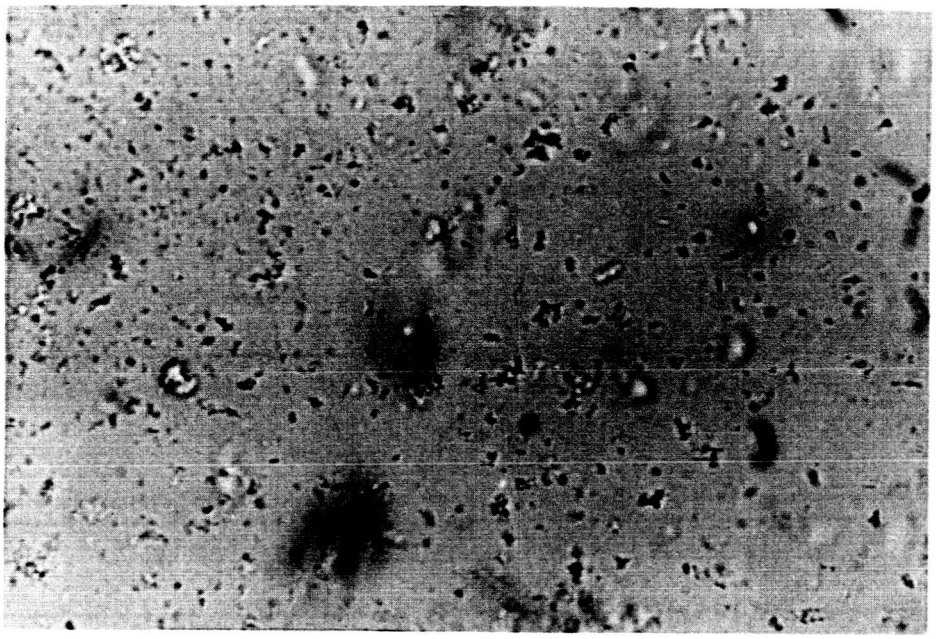

Figure 6: Photomicrograph of SiO_2 Powder Sample (1,695x, Particle Size Range 0.30 - 0.59 microns)

corresponding to the crystalline form, cristobalite; shown in Table 8.

TABLE 8: Characteristics of SiO_2 Powder

Sample	Crystal Structure	Particle Size (microns)
SiO_2	Cubic cristobalite	range 0.5 to 5.0 (optical microscopy)

Spectrochemical analysis of the powder prepared, silicon used, and alumina furnace chamber are shown in Table 9. As for aluminum oxide powders, there was substantial contamination of chromium, iron, nickel, molybdenum and copper believed to come from the transfer line, and aluminum from the reaction chamber.

3.7 Zinc Oxide (ZnO) Powder Preparation

Initial efforts were made to produce a source of zinc vapor by reaction of the metal with the chlorine as was done for aluminum, zirconium, and silicon. The oxide products formed were non-stoichiometric, grey to black powders believed to be zinc rich. The substantial vapor pressure of zinc metal in the chlorinator (zinc vapor pressure is 10^{-1} Torr at 400°C) [10] is believed to account for this result.

Subsequently, zinc vapor was produced directly by heating zinc metal in an aluminum oxide boat; the zinc vapor pressure was controlled by the zinc temperature. At a temperature of 650°C, (where the vapor pressure of zinc is 16 Torr) sufficient zinc vapor was present in the atmosphere for the formation of zinc oxide by the following general reaction:

$$Zn(g) + H_2(g) + 2CO_2(g) \rightleftharpoons ZnO(s) + 2CO(g) + H_2(g) \qquad (12)$$

TABLE 9: Qualitative Spectrochemical Analysis of SiO_2 System

Element	Powder	Source Metal	Reaction Tube
B	1 - 10	ND	ND
Na	ND	ND	$10 - 10^2$
Mg	1 - 10	< 1	$10 - 10^2$
Al	$1 - 10^2$	ND	Remainder Al_2O_3
Si	Remainder SiO_2	Remainder Si	$10^3 - 10^4$
Ca	< 1	ND	$10^3 - 10^4$
Ti	ND	ND	10
V	ND	ND	1
Cr	$10 - 10^2$	ND	10
Mn	< 1	ND	10
Fe	$10 - 10^2$	1 - 10	$10^2 - 10^4$
Ni	< 1	ND	10
Cu	$10 - 10^2$	1 - 10	1
Zn	1 - 10	ND	ND
Mo	$10^2 - 10^4$	ND	ND
Ag	1 - 10	< 1	ND
Cd	$10 - 10^2$	ND	ND
Sn	$10^2 - 10^4$	ND	ND
Hg	ND	ND	1
Pb	ND	ND	10

The zinc metal quickly became coated with oxide, making it difficult to assess the amount of zinc vapor available. The reaction zone temperature was maintained at 1200°C with reaction conditions as shown in Table 10. The amount of zinc evaporated was found to be affected by the total system pressure and reactant gas velocity, indicating that kinetic factors controlled its generation rather than its equilibrium vapor pressure. Conditions used for the formation of zinc oxide powders are also shown in Table 10.

TABLE 10: Conditions for the Production of ZnO Powders

Sample	System Pressure Torr	Temp. °C	Gas Velocity (cm/sec)	Time in Hot Zone (sec)
ZnO	50	1200	40	2.5×10^{-1}
Inputs	CO_2	H_2	Zn(g)	
	.05 ℓpm	.05 ℓpm	.01 ℓpm (estimated)	

3.8 Zinc Oxide (ZnO) Powder Characteristics

The material formed by vapor phase reaction was white in color but showed a wide variation in particle size. This is believed to have resulted from the more difficult and less precise control over the supersaturation ratio than was possible when the metal chlorination system was used. With excess hydrogen in the reactant stream, the product ranged in color from grey to black, but whitened by subsequent firing in an oxygen atmosphere at temperatures above 600°C. Optical examination indicated that the average particle size was 0.25 microns(Fig. 7) The particles had a refractive index

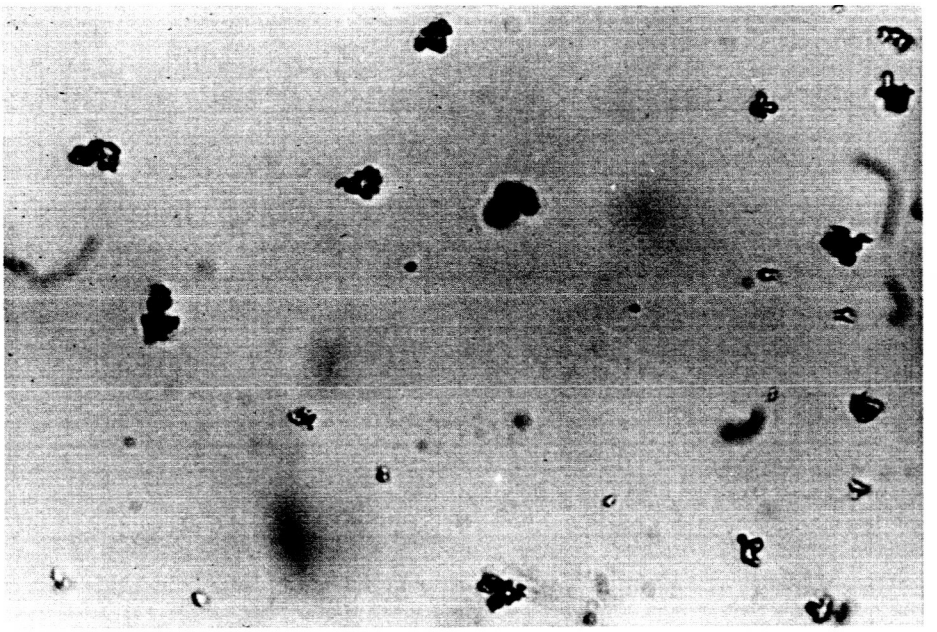

Figure 7: Photomicrograph of ZnO Powder Sample (4,026x; average particle size 0.25 microns)

TABLE 11: Qualitative Spectrochemical Analysis of ZnO Powder (ppm)

Element	Powder	Source Metal	Reaction Tube
B	$10 - 10^2$	ND	ND
Na	ND	ND	$10 - 10^2$
Mg	1 - 10	ND	$10 - 10^2$
Al	$10 - 10^2$	ND	Remainder Al_2O_3
Si	ND	ND	$10^3 - 10^4$
Ca	1 - 10	ND	$10^3 - 10^4$
Ti	ND	ND	10
V	ND	ND	1
Cr	$10 - 10^2$	ND	10
Mn	< 1	ND	10
Fe	1 - 10	50	$10^2 - 10^4$
CO	ND	ND	ND
Mi	1 - 10	ND	10
Cu	$10 - 10^2$	ND	1
As	ND	< 1	ND
Zr	1 - 10	ND	ND
Mo	1 - 10	ND	ND
Ru	1 - 10	ND	ND
Rh	1 - 10	ND	ND
Cd	1 - 10	ND	ND
Sn	$10^2 - 10^3$	ND	ND
Hg	ND	ND	1
Pb	$10^2 - 10^3$	10^2	10

of 2.0. In addition, many platelets and whiskers were formed in the system. They usually appeared growing on the wall of the alumina boat used to contain the zinc metal. These products do not correspond to homogeneous nucleation and growth of powder directly in the vapor phase. A spectrochemical analysis of the oxide powder formed, the zinc metal used as a source material and the furnace tube are shown in Table 11. The lead content, and perhaps the tin content, are substantially greater in the powder than in the starting materials. These constituents presumably result from their greater tendency towards evaporation.

During the homogeneous nucleation of zinc oxide powder, whiskers were formed[11] having a hexagonal morphology and growing up to 4 mm in length, with length to diameter ratios approaching 1250:1. (Fig. 8). Average aspect ratios of 400:1 were measured. The index of refraction of the whiskers was 2.0. Room temperature ultimate tensile strengths up to 9.84×10^5 psi were measured for these whiskers, as shown in Table 12. These measurements were made on a tensile testing machine[12] designed specifically to measure mechanical properties of short whiskers and fibers under axial loads. The instrument provides for horizontal whisker mounting, proper alignment, variable strain-rate testing and instrument read-out.

TABLE 12: Tensile Strength of Vapor-Deposited ZnO Whiskers

Ultimate Tensile Strength (psi)	Cross-Sectional Area (microns^2)
6.63×10^5	5.85
9.84×10^5	5.85
9.32×10^5	10.4

Figure 8: Photomicrograph of ZnO Whiskers
(93x; 1 division equals 20 microns)

3.9 Titanium Dioxide (Rutile, TiO_2) Powder Formation

Titanium tetrachloride was formed by flowing chlorine gas over titanium sponge in the chlorinator (Eq. 13).

$$Ti(s) + 2Cl_2(g) \rightleftharpoons TiCl_4(g) \qquad (13)$$

Rutile powder was produced by homogeneous nucleation using the following general reaction.

$$TiCl_4(g) + 2H_2(g) + 2CO_2(g) \rightleftharpoons TiO_2(s) + 2CO(g) + HCl(g) \qquad (14)$$

Controlled flows of hydrogen and carbon dioxide were reacted with titanium tetrachloride to form titanium dioxide. A reaction zone temperature of 1200°C was maintained to produce the rutile phase of titanium dioxide. The system total pressure was 50 Torr. The external chlorinator temperature was 400°C to insure complete reaction and transfer line temperatures were 200°C which prevented condensation of titanium tetrachloride vapor.

Several exploratory runs were made to establish desirable growth conditions which produced a white powder. Suitable condtions are shown in Table 13.

TABLE 13: Conditions for the Homogeneous Nucleation of TiO_2 Powder

Sample	System Pressure (Torr)	Temp. (°C)	Gas Velocity (cm/sec)	Time in Hot Zone (sec)
TiO_2	50	1200	325	3×10^{-2}
Inputs	H_2	CO_2	$TiCl_4$	
	0.80 (ℓpm)	0.05 (ℓpm)	0.05 (ℓpm)	

3.10 TiO_2 Characteristics

A chemical analysis of the titanium sponge used is shown in Table 14.

TABLE 14: Spectrochemical Analysis of Titanium Metal (all other elements not detected)

Fe	< 100 ppm	Si	< 100 ppm
Mg	< 25	Mn	< 25
Sn	< 100	V	< 50
Na	980		

The production of rutile powder was primarily to establish growth parameters for the preparation of zinc titanate. A white powder was produced with refractive index greater than 2.2. The average particle size was 0.59 microns diameter (Figure 9). During the course of regular rutile runs, rutile fibers and platelet were discovered growing outside of the isothermal hot zone. Lower supersaturation was present in this lower temperature region which favored growth of rutile fibers. Figure 10 is a photomicrograph of a representative sample of these fibers and platelets.

3.11 Zinc Titanate ($ZnTiO_3$) Powder Formation

Zinc titanate powder was produced by combining the method of producing zinc oxide with that of producing rutile powder. Conditions had been previously established during this study that allowed both the production of zinc oxide and titanium dioxide at a reaction zone temperature of 1200°C and a total system pressure of 50 Torr. From previous experience with zinc oxide, an excess of hydrogen was not used. Several runs were made and inputs determined were hydrogen,

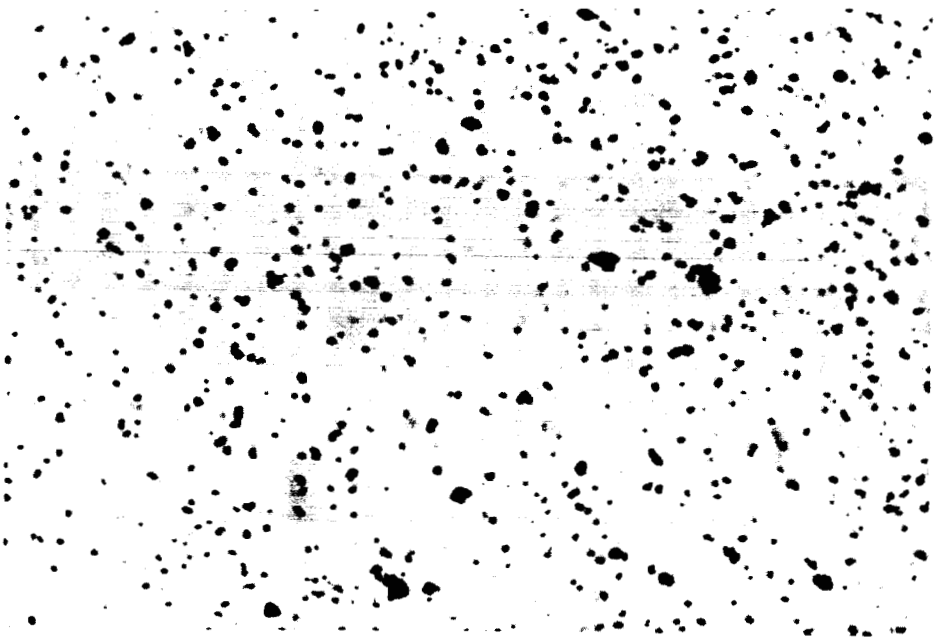

Figure 9: Photomicrograph of TiO_2 Powder Sample (1,695x; average particle size 0.59 microns)

Figure 10: Photomicrograph of TiO_2 Fibers and Platelets (93x; 1 division equals 20 microns)

0.90 liters/minute; carbon dioxide, 0.10 liters/minute; titanium tetrachloride, 0.05 liters/minute and zinc vapor, 0.01 liters/minute (estimated). Conditions are listed in Table 15.

TABLE 15: Conditions for the Production of $ZnTiO_3$ Powder

Sample	System Pressure (Torr)	Temp. (°C)	Gas Velocity (cm/sec)	Residence in Hot Zone (sec)
$ZnTiO_3$	50	1200	382	2.6×10^{-2}
Input (ℓpm)	H_2	CO_2	Zn	$TiCl_4$
	.9	.1	.01	.05

When a powder fall of rutile was observed, zinc vapor was introduced by heating the alumina boat containing zinc metal to 650°C. The reaction proceeded until a quantity of white powder was produced. The particle size ranged from 2.5 to less than 0.5 microns as seen in Fig. 11. This powder was examined by x-ray diffraction to determine its crystal structure. As shown in Fig. 12, the major phase was found to be TiO_2 (rutile). Although no data for $ZnTiO_3$ is available in the ASTM card index, a comparison of the lines of the minor constituent with the patterns of $MgTiO_3$ and $CoTiO_3$ agree fairly well. Based on this comparison the minor constituent is probably $ZnTiO_3$. At 1200°C, $ZnTiO_3$ is not stable as an equilibrium phase, since it dissociates at 945°C to form Zn_2TiO_4 and TiO_2. Thus, a mixture of TiO_2 and $ZnTiO_4$ was probably formed at 1200°C and partially transformed into $ZnTiO_3$ on cooling.

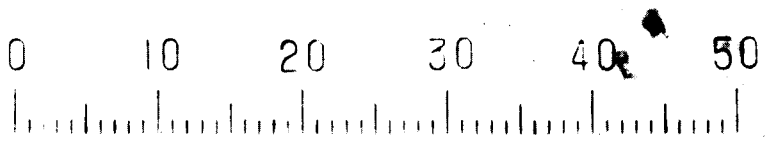

Figure 11: Photomicrograph of $ZnTiO_3$ and TiO_2 Powder Sample (745x; 1 division equals 2.5 microns)

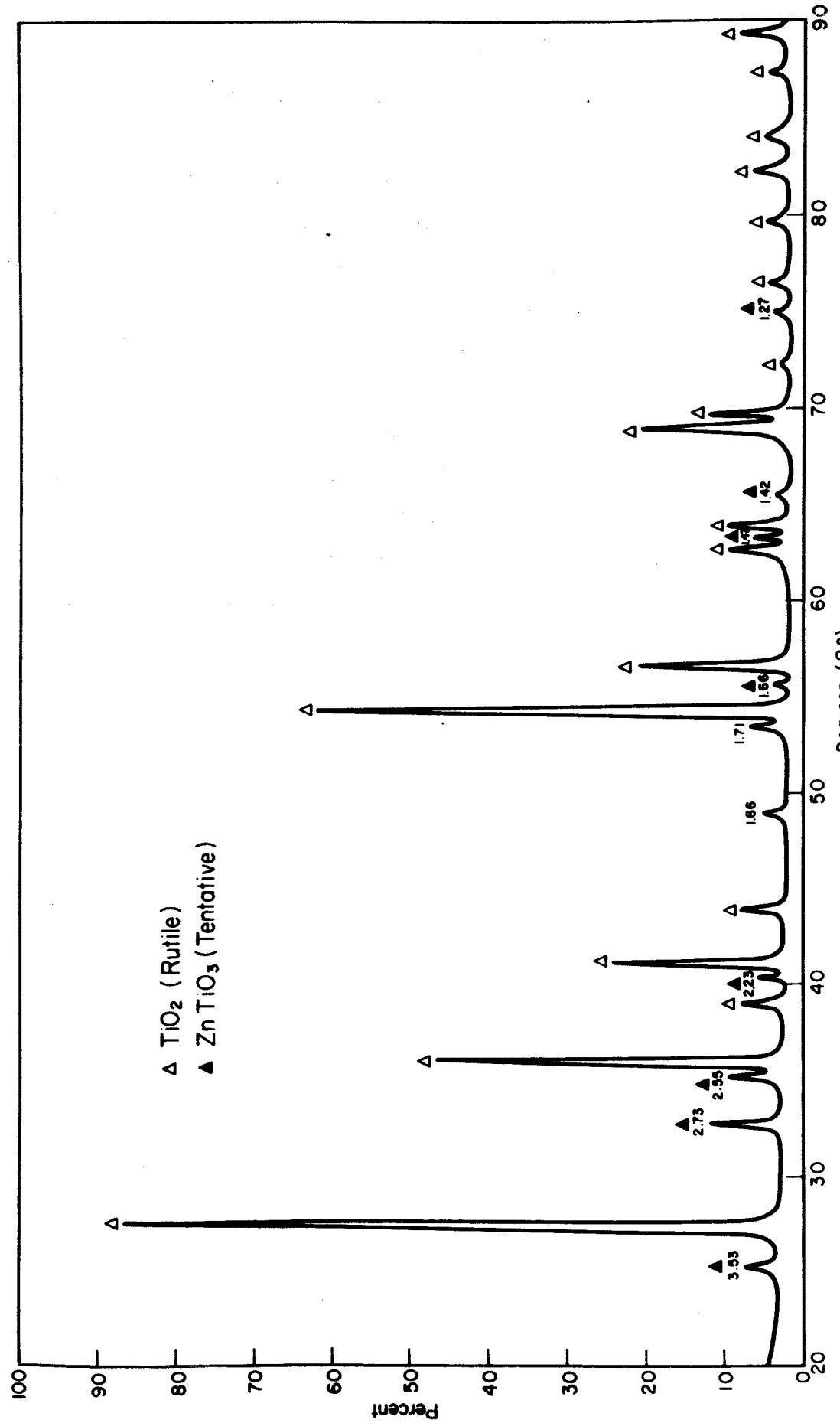

Figure 12: X-Ray Diffraction Pattern of $ZnTiO_3$ and TiO_2 Powder Sample.

3.12 Zinc Titanate Characteristics

Table 16 compares purities of starting materials, reaction chamber and powder. A reduction in magnesium, manganese, iron, calcium vanadium and sodium concentrations over the starting material is noted. The impurity level in the zinc titanate powder for some elements has remained consistent with impurity content in the starting materials; namely, nickel, chromium, lead, tin and silicon. Boron, copper and molybdenum have contaminated the sample probably from contact with system components.

The sample was examined by optical microscopy to determine particle size, which ranged from below 0.5 microns to 2.5 microns. The major constituent of the white powder produced was TiO_2 (rutile) intermixed with $ZnTiO_3$ (zinc titanate).

TABLE 16: Qualitative Spectrochemical Analysis of $ZnTiO_3$ Powder (ppm)

Element	Powder	Source Metal		Reaction Chamber
		Ti	Zn	
B	$10 - 10^2$	ND	ND	ND
Na	ND	980	ND	$10 - 10^2$
Mg	< 1	< 25	ND	$10 - 10^2$
Al	1 - 10	ND	ND	Remainder Al_2O_3
Si	$10 - 10^2$	< 100	ND	$10^3 - 10^4$
Ca	ND	ND	ND	$10^3 - 10^4$
Ti	Remainder $ZnTiO_3$	Remainder Ti	ND	10
V	ND	< 50	ND	1
Cr	1 - 10	ND	ND	10
Mn	< 1	< 25	ND	10
Fe	1 - 10	< 100	50	$10^2 - 10^4$
Mi	1 - 10	ND	ND	10
Cu	10 - 100	ND	ND	1
Zn	Remainder $ZnTiO_3$	ND	Remainder Zn	ND
As	ND	ND	< 1	ND
Zr	$10 - 10^2$	ND	ND	ND
Mo	1 - 10	ND	ND	ND
Ag	< 1	ND	ND	ND
Cd	< 1	ND	ND	ND
Sn	$10^2 - 10^3$	< 100	ND	ND
Pb	$10 - 10^2$	ND	100	10

4.0 CONCLUSIONS

The feasibility of producing powders of aluminum oxide, zirconium dioxide, silicon dioxide, titanium dioxide, and zinc oxide by a vapor phase reaction process was determined. Zinc titanate powder was probably formed, but only in association with TiO_2. Appropriate parameters for controlling the formation of individual powders were determined, but no effort was made to establish optimum conditions for particular particle size and powder characteristics.

As a result of high gas velocities and short growth times, remarkably uniform particle sizes were achieved by the vapor phase growth process. This is one of the unique and valuable features of the process.

Purity levels of powders produced by gas phase reactions were fixed by the composition of the starting material, by interaction with the furnace chamber, and by contamination from vapor transfer lines. This indicates that considerable care is required for the preparation of extremely pure powder. At the same time, it demonstrates that desired amounts of doping constituents of a wide range of elements can be successfully incorporated in the powder formed.

A series of experiments with aluminum oxide indicated that by control of temperature and gas velocity, which control the particle growth rate and growth time, particle size ranges can be attained having uniform particle diameters ranging from a few hundredths of a micron to a few microns.

5.0 REFERENCES

1. W. B. Campbell, "Feasibility of Forming Al_2O_3 and B Whiskers Vapor Phase Reactions", final report, Contract DA-19-020-AMC-0068(X), 1965.

2. W. B. Campbell, "Continuous Whisker Formation", Chemical Engineering Progress, 62, (3) 1966.

3. W. B. Campbell and W. D. Kingery, "Optical Control of Vapor Phase Crystal Growth", U. S. Patent Application 490,935 (1965).

4. P. S. Schaffer, "Vapor Deposition Growth of Oxide Single Crystals from Metal Halides", final report, Contract Nonr-4574(00), 1965.

5. J. P. Hirth and G. M. Pound, Condensation and Evaporation, McMillan, N. Y., p. 15 (1963).

6. P. S. Schaffer, "Vapor Phase Growth of Alpha-Alumina Single Crystals", J. Amer. Ceram. Soc., 48 (10) 508-11 (1965).

7. C. E. Wicks and F. E. Block, "Thermodynamic Properties of 65 Elements - Their Oxides, Halides, Carbides and Nitrides", Bull. 605, Bur. of Mines (1963).

8. D. Gates, National Aeronautics and Space Administration, private communication.

9. Jarrell-Ash Company, Waltham, Massachusetts

10. An. N. Nesmayanov, Vapor Pressure of the Elements, Academic Press, N. Y. (1963).

11. P. S. Schaffer, D. W. Jones and L. E. Tagliani, "Vapor Phase Growth of ZnO Whiskers", submitted for publication (1966).

12. R. C. Folweiler, "Tensile Test Apparatus", U. S. Patent Application 486,170 (1965).

13. F. H. Dulin and D. E. Rase, J. Amer. Ceram. Soc., 43 (3) 130 (1960).

ACKNOWLEDGMENT

The authors wish to acknowledge the preparation of some of the powder photographs by Dr. Stanley Cortell of Walter Reed Army Medical Center.

6.0 APPENDIX: Tabulated Powder Preparation Conditions Used in These Investigations

6.1 Al_2O_3 (Alumina)

Conditions for the growth of alumina powder in a 5.5 cm inside diameter furnace are tabulated below:

1. Reaction zone temperature 1750°C
2. Chlorinator temperature 400°C
3. $AlCl_3$ transfer lines 220°C
4. System total pressure 50 Torr
5. Gas flows

$CO_2(g)$	$CO(g)$	$H_2(g)$	$AlCl_3(g)$
0.20 ℓpm	0.80 ℓpm	0.80 ℓpm	0.12 ℓpm

6.2 ZrO_2 (Zirconium Dioxide)

1. Reaction zone temperature 1550°C
2. Chlorinator temperature 400°C
3. $ZrCl_4$ transfer lines temperature 400°C
4. System total pressure 60 Torr
5. Gas flows

$CO_2(g)$	$CO(g)$	$H_2(g)$	$ZrCl_4(g)$
.05 ℓpm	0.30 ℓpm	.90 ℓpm	.05 ℓpm

6.3 SiO_2 (Silicon Dioxide)

1. Reaction zone temperature 1550°C
2. Chlorinator temperature 400°C
3. $SiCl_4$ transfer line temperature 200°C
4. System total pressure 60 Torr
5. Gas flows

$H_2(g)$	$CO_2(g)$	$SiCl_4(g)$
.90 ℓpm	.03 ℓpm	.05 ℓpm

6.4 ZnO (Zinc Oxide)

1.	Reaction zone temperature	1200°C
2.	Zinc vapor source temperature	650°C
3.	System total pressure	50 Torr
4.	Gas flows	

CO_2	$H_2(g)$	Zn(g)
0.05 ℓpm	0.05 ℓpm	0.01 ℓpm*

6.5 TiO_2 (Titanium Dioxide)

1.	Reaction zone temperature	1200°C
2.	Chlorinator temperature	400°C
3.	$TiCl_4$ transfer line temperature	200°C
4.	System total pressure	50 Torr
5.	Gas flows	

$H_2(g)$	$CO_2(g)$	$TiCl_4(g)$
0.80 ℓpm	0.05 ℓpm	.05 ℓpm

6.6 $ZnTiO_3$ (Zinc Titanate)

1.	Reaction zone temperature	1200°C
2.	Chlorinator temperature	400°C
3.	$TiCl_4$ transfer line temperature	200°C
4.	Zinc vaporizer temperature	650°C
5.	System total pressure	50 Torr
6.	Gas flows	

$H_2(g)$	$CO_2(g)$	Zn*	$TiCl_4(g)$
0.90 ℓpm	0.10 ℓpm	0.01 ℓpm	0.05 ℓpm

*estimated from vapor pressure of Zn.